

Single-top-quark production in the tW^\pm channel and Higgs boson signals via $H \rightarrow W^+W^-$ at the CERN Large Hadron Collider

Stefano Moretti*

Cavendish Laboratory, University of Cambridge, Madingley Road, Cambridge, CB3 0HE, United Kingdom

(Received 27 May 1997)

In a recent study by Dittmar and Dreiner it was shown that with appropriate selection cuts the signature of events containing two charged leptons and missing energy represents the best chance of detecting the standard model Higgs scalar in the mass range between 155 and 180 GeV, the primary decay of the Higgs boson being into pairs of charged gauge bosons. The largest background to this channel is due to irreducible W^+W^-X production. In the present paper we calculate the contribution of events of the type $bg \rightarrow tW^\pm \rightarrow bW^+W^- \rightarrow b\ell^+\ell'^-\nu_\ell\bar{\nu}_{\ell'}$, which have not been considered yet within the new selection strategy. We show that the yield of this background is rather large, at the level of that produced by W^+W^- , $t\bar{t}$, or tbW^\pm events, and thus needs to be incorporated in future experimental analyses. However, we find that its inclusion will not spoil the possibilities of Higgs boson detection in the above-mentioned channel at the CERN Large Hadron Collider. [S0556-2821(97)04123-4]

PACS number(s): 14.80.Bn, 13.38.Be, 13.85.Hd, 14.65.Ha

I. INTRODUCTION AND MOTIVATION

In a recent paper by Dittmar and Dreiner [1] (see also Ref. [2]) it was pointed out that the signature of events with two charged leptons and missing energy or momentum at the CERN Large Hadron Collider (LHC) represents the best chance of detecting the standard model (SM) Higgs boson in the mass range $155 \text{ GeV} \leq M_H \leq 180 \text{ GeV}$. In Ref. [1], simple selection criteria were outlined, which should allow one to extract the Higgs boson decay channel $H \rightarrow W^+W^-$ from the nonresonant W^+W^-X production (where X represents possible additional particles in the final state) with a signal-to-background ratio of about one to one, thus allowing a $(5-10)\sigma$ detection with only 5 inverse picobarns of integrated luminosity $\mathcal{L} = \int L dt$. The appealing prospect is that this significance can be achieved in less than one year of running of the CERN machine at the initial low luminosity $L = 10^{33} \text{ cm}^{-2} \text{ sec}^{-1}$. Indeed, this is a clear improvement compared to the Higgs boson search strategy based on the decay mode $H \rightarrow ZZ^* \rightarrow$ four charged leptons, which was the detection channel exploited even in the most recent experimental simulations [3,4] for the mentioned Higgs boson mass range. This is evident if one considers that in order to disentangle a 5σ signal in the latter case at least 100 fb^{-1} are required.

The first studies of the $H \rightarrow W^+W^-$ decay mode [5,6] in the context of Higgs boson searches at the LHC date back to Ref. [7] and to the 1990 Workshop [8] for a LHC with $\sqrt{s} = 16 \text{ TeV}$. Further analyses were subsequently performed, in Ref. [9]. In various instances, also several signal-to-background studies were carried out (see Sec. 2 of Ref. [1] for a review). The unanimous conclusion was that the $H \rightarrow W^+W^- \rightarrow \ell^+\ell'^-\nu_\ell\bar{\nu}_{\ell'}$ channel (with $\ell, \ell' = e, \mu$) should provide a useful tool to detect the Higgs boson in the mentioned mass range, though more appropriate analyses

(including hadronization and detector effects) were recognized to be needed to support those (mostly parton level) results.

This was done in Ref. [1], by using the Monte Carlo (MC) program PYTHIA [10]. Further refinements were also introduced there, which were not included in the previous literature. Namely, (i) the inclusion of $W^\pm \rightarrow \tau^\pm \nu_\tau \rightarrow \ell^\pm \nu_\ell \nu_\tau$ decays (with $\ell = e, \mu$), (ii) the simulation of the background due to $gg \rightarrow tbW^\pm$ events [11,12], and (iii) cuts previously employed [7,9] were further supported by new constraints, introduced mainly in order to discriminate against the ‘‘irreducible’’ background from continuum production of W^+W^-X events.

It is the purpose of this paper to provide additional material to motivate the exploitation of the $H \rightarrow W^+W^-$ channel in Higgs boson searches at the LHC, as we have studied the irreducible background due to

$$bg \rightarrow tW^\pm \rightarrow bW^+W^- \rightarrow b\ell^+\ell'^-\nu_\ell\bar{\nu}_{\ell'} \oplus \text{c.c.}, \quad (1)$$

‘‘single-top-quark’’ events via bg fusion (also called ‘‘ tW^\pm production’’), which was not considered in Ref. [1], and we will show that this can be reduced to a manageable level by the same selection criteria recommended in [1]. In fact, for completeness, we have also computed the yield of the process

$$bg \rightarrow bW^+W^- \rightarrow b\ell^+\ell'^-\nu_\ell\bar{\nu}_{\ell'} \oplus \text{c.c.}, \quad (2)$$

involving all the tree-level graphs producing the final state $b\ell^+\ell'^-\nu_\ell\bar{\nu}_{\ell'}$: that is, not only the single-top-quark ones isolated in reaction (1), but also all the other diagrams contributing at the perturbative order¹ $O(\alpha_{\text{em}}^4 \alpha_s)$.

¹The symbol $\oplus \text{c.c.}$ means that we have calculated also the charged conjugated processes initiated by $\bar{b}g$ scatterings and these are included in all event rates presented in the following sections.

*Electronic address: moretti@hep.phy.cam.ac.uk

With respect to the analysis performed in Ref. [1], we will adopt two simplifications, which we believe will not spoil the validity of our conclusions. First, although we will implement the same cuts considered in Ref. [1], we will confine ourselves to the parton level only. However, since at lowest order the final states of reactions (1) and (2) involve only one hadronic system (i.e., the b quark fragmenting into hadrons), whereas the Higgs signal $H \rightarrow W^+ W^- \rightarrow \ell^+ \ell'^- \nu_\ell \bar{\nu}_{\ell'}$ is purely leptonic, we expect the effects of hadronization not to modify drastically the parton level dynamics. Second, we will only discuss the channels $W^+ W^- \rightarrow \ell^+ \ell'^- \nu_\ell \bar{\nu}_{\ell'}$, with $\ell, \ell' = e, \mu$, thus neglecting the case of W^\pm decays into tau leptons via the three-body channels $W^\pm \rightarrow \tau^\pm \nu_\tau \rightarrow \ell^\pm \nu_\ell \nu_\tau$. This is done to simplify the description at parton level [especially in the case of the complete process (2)], as in this way we can avoid to calculate complicated two-to-seven- and two-to-nine-body subprocesses. In practice, contributions involving τ decays amount to $\approx 1.9\%$ of the total $\approx 7\%$ leptonic branching ratio of $W^+ W^-$ pairs, so that the bulk of the produced $W^+ W^-$ events are indeed included in our study. In general, we stress that we are here only interested in the relative rates of signal and background and we expect that the implementation of a full Monte Carlo simulation and the inclusion of the $W^\pm \rightarrow \tau \nu_\tau$ decays will presumably affect both in a rather similar manner.

The reason for studying processes (1) and (2) as a potential background in Higgs boson searches in the two leptons plus missing energy channel is that single-top-quark production via process (1) has very large event rates at the LHC, as its total cross section amounts to 55–60 pb at $\sqrt{s} = 14$ TeV (see later on), thus being comparable to that of the process $gg \rightarrow tbW^\pm$ considered in Ref. [1] (see, e.g., Refs. [12,13]).² Furthermore, we stress that compared to the final state tbW^\pm , which eventually yields the signature $b\bar{b}W^+W^-$, that of reaction (1) [and, more generally, of the complete process (2)] can boast only one additional particle with respect to the Higgs signature (this rendering its reduction less effective than that of tbW^\pm events, which have two additional jets³). In fact, the latter is produced at lowest-order via gluon-gluon fusion into an on-shell Higgs boson, through a top quark loop [14]: $gg \rightarrow H \rightarrow W^+ W^- \rightarrow \ell^+ \ell'^- \nu_\ell \bar{\nu}_{\ell'}$. However, we notice that the K factor of Higgs boson production via gg fusion has been shown to be very large, around two [15–17] in the mass range $155 \text{ GeV} \leq M_H \leq 180 \text{ GeV}$ (and outside, as well [18]). In particular, a large component of the next-to-leading (NLO) order corrections to the gluon-gluon fusion mechanism of Higgs production is due to the real radiation

²Note that the leading order (LO) rates of the $gg \rightarrow H$ signal for $155 \text{ GeV} \leq M_H \leq 180 \text{ GeV}$ vary between 10 and 8 pb, approximately.

³In this respect, we should mention that an extensive compilation and a detailed discussion of processes involving single-top-quark production at hadron colliders has recently been given [12]. In particular, according to the classification of Ref. [12], there are six of these different hard parton scatterings. However, process (1) is the only one contributing at lowest order to the irreducible background $W^+ W^- X$ with one additional particle in the final state (i.e., $X \equiv b$), as the others always produce a second (light) jet.

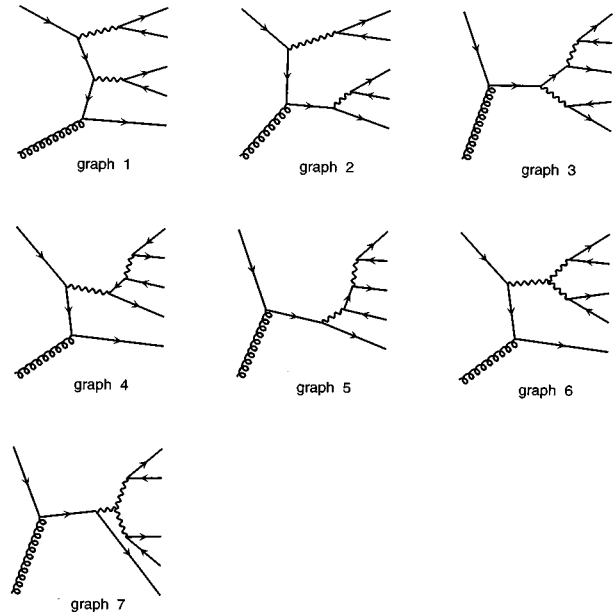


FIG. 1. Feynman diagram topologies contributing at the tree level to the process $bg \rightarrow b\ell\ell'\nu_\ell\nu_{\ell'}$, where ℓ represents a lepton. Internal wavy lines represent a photon, a Z , or a W^\pm , whereas the internal solid ones refer to a lepton, a neutrino, a bottom quark, or a top quark, as appropriate. The total number of graph is 43 (excluding Higgs couplings). The single-top-quark diagrams are Nos. 2 and 3. Charge-conjugated diagrams can be trivially obtained by reversing the fermion lines.

[18] of a quark or gluon, so that also signal events are naturally accompanied by an additional detectable jet inside the detectors.

For reference, we recall that the matrix element of process (1) was already computed in Ref. [19] and first studied in the context of Higgs boson searches (and of $W^+ W^-$ physics, as well) in Ref. [20] (for its relevance in the case of top quark physics, see Ref. [12]). However, only the invariant mass region $M_{\ell W} \equiv \sqrt{s} > 850 \text{ GeV}$ was considered there, as a background to signatures of heavy Higgs bosons decaying into longitudinal polarized $W^+ W^-$ pairs [21].

The plan of this paper is as follows. In the next section we give some details of the calculation. Section III is devoted to a discussion of the results. Our conclusions are in Sec. IV.

II. CALCULATION

The tree-level Feynman “topologies” that one needs for computing processes (1) and (2) are given in Fig. 1. Once all the internal propagator are correctly inserted, one gets a total of 43 Feynman graphs [the single-top-quark diagrams pertaining to reaction (1) can be obtained from the topologies 2 and 3]. To calculate the corresponding amplitude squared, we have used MADGRAPH [22] and HELAS [23]. The integrations over the appropriate phase spaces have been performed by using VEGAS [24]. The codes produced have been carefully checked for gauge and Becchi-Rouet-Stora (BRS) [25] invariance. Furthermore, the total cross section for process (1), obtained by selecting the only two graphs with on-shell top quark production out of those displayed in Fig. 1, has been compared against the results given in Ref. [12] for the Tevatron and in Ref. [20] for the Superconducting Super

Collider (SSC), with identical choice of parameters, cuts (where applied), and structure functions, and perfect agreement has been found. The signal rates have been computed by using the program already adopted in Refs. [26,27]. However, contrary to the case of Ref. [26] where NLO rates were used to calculate the Higgs production cross sections via gg fusion, and in line with Refs. [1,27], we have used here the LO results. This has been done for consistency, as one-loop calculations do not exist to date for processes (1) and (2). It is, however, important to point out that whereas the complete corrections to the main Higgs production process via gluon-gluon fusion are large and positive [18], those to the single-top-quark process (1) are expected to be much smaller [12].

The b quark in the initial state of reactions (1) and (2) has been treated as a constituent of the proton with the appropriate momentum fraction distribution $f_{b/p}(x, Q^2)$, as given by the parton distribution functions (PDF's). As a default set of the latter, we have used Martin-Roberts-Sterling set A [MRS(A)] [28]. However, as the PDF's of the gluon inside the proton are not so well known at medium and small x and since those of b quarks suffer from potentially large (theoretical) uncertainties (see, e.g., Ref. [29]), we have produced our results in the case of other four sets of recent NLO structure functions, which give excellent fits to a wide range of deep inelastic scattering data (including the latest measurements from the DESY ep collider HERA) and to data on other hard scattering processes. These are the packages MRS (A', G, R1, R2) [28,30,31]. The QCD strong coupling α_s entering explicitly in the production cross sections and implicitly in the parton distributions has been evaluated using the CERNLIB package at the scale $\mu = \sqrt{s}$ (i.e., the c.m. energy at parton level). We will discuss the μ dependence of the LHC rates in the following section. Indeed, one should remember that also the value of α_s associated with each parton set represents in principle a residual source of error in the predictions of the different PDF's. However, the value adopted in each set is chosen to match the data during the extraction, so that we do not expect α_s to be a significant source of uncertainty.

In the numerical calculations we have adopted the following values for the electromagnetic coupling constant and the weak mixing angle: $\alpha_{\text{em}} = 1/128$ and $\sin^2 \theta_W = 0.2320$. For the gauge boson masses and widths, we have taken $M_Z = 91.1888$ GeV, $\Gamma_Z = 2.5$ GeV, $M_{W^\pm} \equiv M_Z \cos \theta_W \approx 80$ GeV, and $\Gamma_{W^\pm} = 2.08$ GeV, while for the top quark mass we have used $m_t = 175$ GeV [32]. All other fermions have been considered massless, including the b quark. In particular, the choice $m_b = 0$ has been maintained also in the Yukawa couplings of the theory. In this way, no diagram involving radiation of Higgs bosons off the b lines has been included in process (2). For simplicity, we have set the Cabibbo-Kobayashi-Maskawa (CKM) matrix element of the top-bottom quark coupling equal to 1. In this respect, we recall again Ref. [12], where it was shown that off-diagonal CKM matrix element subprocesses are negligible at the Tevatron. We do expect the same to occur at LHC regimes.

Finally, as total c.m. energy of the colliding beams at the LHC, we have adopted the value $\sqrt{s} = 14$ TeV.

III. RESULTS

Our results are presented in Table I and Figs. 2–6. Note that for the time being we assume that no b -tagging identi-

fication is exploited in events of the types (1) and (2). The integrated luminosity adopted throughout the paper will be 5 fb^{-1} .

A. Selection cuts

As event selection procedure, we have adopted the same one exploited in Ref. [1], to which we refer the reader for a detailed discussion concerning the meaning of the various cuts. We only tabulate these here, in order to introduce a notation that will be used in the remainder of this paper (note that the two leptons ℓ and ℓ' must be of opposite sign). Following the same numerical sequence as in [1], we ask (at parton level) the following: (1) $p_T^{\ell, \ell'} > 10$ GeV, p_T^ℓ or $p_T^{\ell'} > 20$ GeV, $\theta_{\ell, \ell'} > 10^\circ$, for the transverse momentum and the separation angle of the two leptons; (2) $|\eta^{\ell, \ell'}| < 2$, for the pseudorapidity of the two leptons; (3) $E_b < 5$ GeV if $\theta_{b, \ell, \ell'} < 20^\circ$, for the energy of the b quark and the separation angles between the leptons and the b quark; (4) $M_{\ell\ell'} < 80$ GeV, for the dilepton mass; (5) $p_T^{\text{miss}} > 20$ GeV, for the missing transverse momentum of the event; (6) $\phi < 135^\circ$, for the angle between the two leptons in the plane transverse to the beam direction; (7) if $|\eta^b| < 2.4$, then $p_T^b < 20$ GeV, for the transverse momentum and the pseudorapidity of the b quark; (8) $|\cos \theta| < 0.8$, for the cosine of the dilepton system with respect to the beam direction; (9) the enforcement $10^\circ < \phi < 45^\circ$, for the same angle defined in (6); (10) $M > 140$ GeV, for the estimated invariant mass of the W^+W^- system; (11) $0 < \cos \xi < 0.3$, for the angle between the lepton with the largest transverse momentum, boosted to the dilepton rest frame, and the momentum vector of the dilepton system.

A few comments are in order before proceeding further, concerning the application of cuts (3) and (7). As for cut (3), according to our parton level implementation, background events are rejected if the b quark is energetic and is found near one of the leptons. On the one hand, we certainly expect the b quark to be very fast. On the other hand, we do not see *a priori* any reasons why the quark and leptons should be created in collinear configurations. This is in fact confirmed by the spectra given in Fig. 2(a). However, things would look quite different at hadron level. In fact, the jet produced by the bottom quark would have a finite size and the hadrons produced in the showering would carry only a fraction of the original parton energy. Although we miss these two aspects, we stress that the two systematics errors we introduce with our treatment do work in opposite directions, so as to counterbalance each other. Cut (7) will have no effect on our signal rates, as we are considering here neither τ -decay modes nor initial state QCD radiation, whereas for the background it will act directly on the b parton. This corresponds to an overestimate of the signal, while we believe that the accepted fraction of background events will be predicted accurately, as the efficiency in reconstructing the b momentum from the hadrons should be rather high because of the clean environment (the two leptons) in which the b quark fragments. Whichever is the interplay between parton and hadron levels, it is anyway clear that it is cut (7) that will introduce a strong reduction factor on the background, as the b jet will

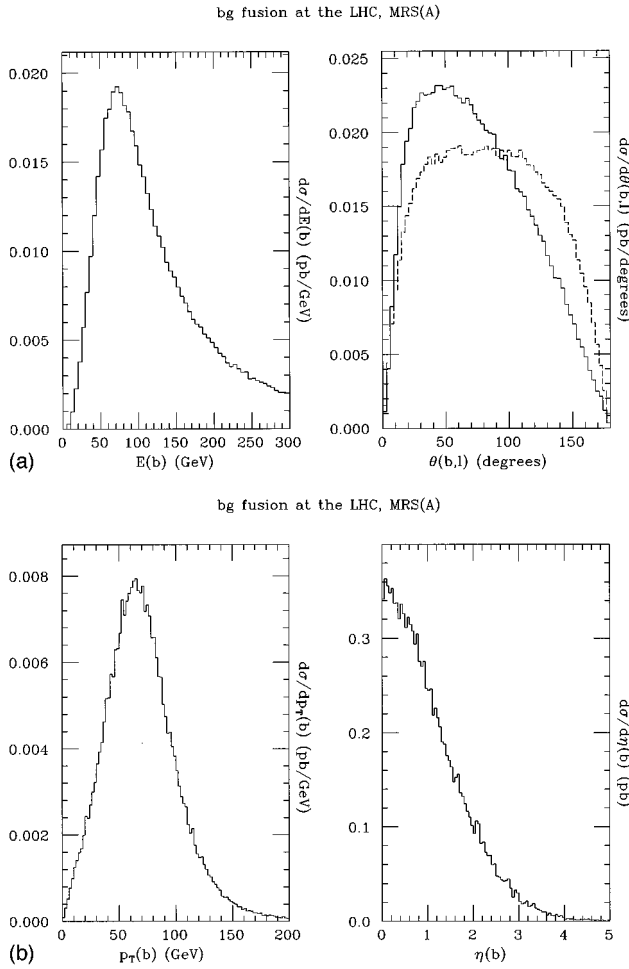


FIG. 2. Differential distributions in (a) energy of the final state b jet (left plot) and its angular separation from the two leptons (right plot: from that generated by the top quark decay W^\pm , solid line, and from that generated by the non-top-quark decay W^\pm , dashed line) and (b) transverse momentum (left plot) and pseudorapidity (right plot) of the final state b jet in events of the type $bg \rightarrow tW^\pm \rightarrow bW^+W^- \rightarrow b(\ell^-\bar{\nu}_\ell)(\ell'^+ \nu_{\ell'})$, with $\ell, \ell' = e, \mu$, at the LHC, (a) before the acceptance cuts and (b) after the acceptance cuts (1)–(6). The parton distribution functions used are MRS(A).

be easily detectable in pseudorapidity and will also have a large transverse momentum⁴ [see Fig. 2(b)].

B. Theoretical error

As a first step of our analysis, we have compared the production rates of process (1) and (2) and found that in Higgs boson searches [that is, for the selection cuts (1)–(11)] the additional contributions from the non-top-quark diagrams of Fig. 1 are negligible. Therefore, in the following we will neglect them.

As one of the possible means of estimating the uncertainty of the theoretical predictions on the gluon distribution (and hence the b one), we have calculated the cross section

⁴Note that Fig. 2(b) has been plotted after having already implemented the constraints (1)–(6), and so will be in all forthcoming figures.

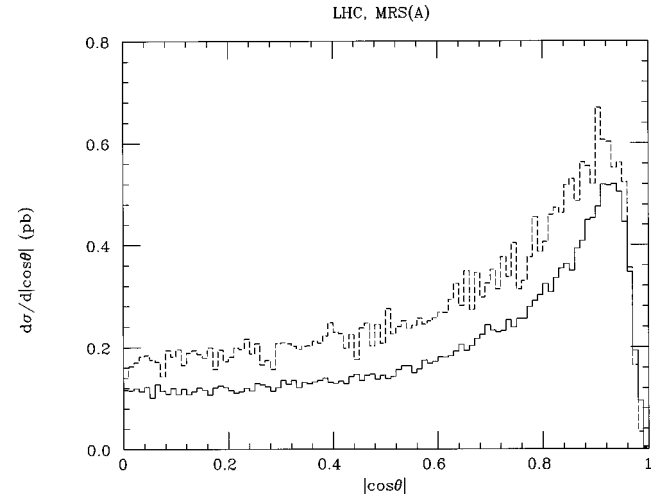


FIG. 3. Differential distributions in the polar angle of the dilepton system with respect to the beam direction for the Higgs signal ($M_H = 170$ GeV, solid histogram) and the single-top-quark background (dashed histogram) at the LHC after the acceptance cuts (1)–(6). The parton distribution functions used are MRS(A). Note that the background rates have been divided by 2 in order to facilitate the comparison between the two curves.

for on-shell single-top-quark production via the two-to-two body process $bg \rightarrow tW^\pm \oplus$ c.c. for the mentioned five sets of PDF's. The spread around the value obtained from MRS(A) (the set that we will adopt as a default in the following) is between -9% [from MRS(G)] and $+3\%$ [from MRS(R2)]. This will represent throughout the paper the conservative estimate at present time of the uncertainty on the bg -fusion cross section into single top quarks due to the parton distributions. Note that the above values roughly compare to those identified (for the same sets) in Ref. [26] for the case of gg fusion into an on-shell Higgs boson, so that this helps in this context in carrying out a consistent signal-to-background analysis.

Finally, the factorization scale dependence (which quantifies our ignorance of higher order corrections) of the background rates via process (1) has been estimated by varying μ in the range $\sqrt{s}/2 < \mu < 2\sqrt{s}$ when calculating the total cross section. We notice that, using MRS(A), differences with respect to the rate at $\mu = \sqrt{s}$ are less than 0.1% at $\mu = \sqrt{s}/2$ and -3% at $\mu = 2\sqrt{s}$. We have verified that similar effects also occur when other PDF's are used. Such numbers are rather small and presumably comparable with the experimental uncertainties.⁵

C. Kinematics and event rates

One should expect the impact of the cuts (8) and (9) to be similar on both signal and background, as can be noticed from Figs. 3 and 4, respectively. In fact, the shapes of the

⁵Note that the scale dependence of processes producing the final state $tW^\pm X$ at the Tevatron has been studied in Ref. [12], where variations between -14% and $+20\%$ were quoted, for μ spanning over the range between $\mu = m_t/2$ and $2m_t$.

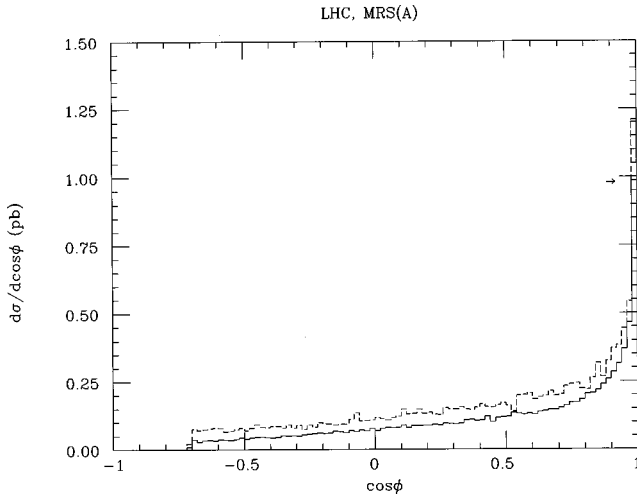


FIG. 4. Differential distributions in the azimuthal angle of the dilepton system in the plane transverse to the beam direction for the Higgs signal ($M_H=170$ GeV, solid histogram) and the single-top-quark background (dashed histogram) at the LHC after the acceptance cuts (1)–(6). The parton distribution functions used are MRS(A). Note that the background rates have been divided by 2 in order to facilitate the comparison between the two curves.

corresponding distributions are almost identical.⁶

Not even the invariant mass M of the reconstructed (from the lepton and the missing momenta) W^+W^- system is helpful to discriminate the signal from the background (see Fig. 5). In fact, the background spectrum is almost entirely beyond the minimum value of 140 GeV implied by cut (10). The discrimination power of such constraint is thus very limited, if not self-defeating.

The only cut among those introduced in Ref. [1] to reduce the irreducible W^+W^-X background from W^+W^- , tt , and tbW^\pm events which is also effective against $bg \rightarrow tW^\pm$ is cut (11), as can be appreciated from Fig. 6. In fact, the two charged leptons from the background have a rather large angular spread, so that the maximum of the background distribution is located around the value 0.6.

The accepted event rates, for both signal and background, for a selection of six Higgs boson masses, are presented in Table I ($\sqrt{s}=14$ TeV and $\mathcal{L}=5$ fb⁻¹). When comparing the numbers in Table I one should bear in mind that the background rates there should be added to those given in Table II of Ref. [1]. This should, however, be done after treating all background sources in W^+W^-X events on the same footing (i.e., consistently at the parton or, better, hadron level). This is beyond our intentions and capabilities, our aim here being to make the point that background events from process (1) are large compared to the signal, as they vary between 11% and 22% of the Higgs rates, depending on the mass of the scalar. Therefore, their effect in the signal-to-background significance is of the same order as that of any of the three processes $pp \rightarrow W^+W^-$, $pp \rightarrow t\bar{t}$, and $pp \rightarrow tbW^\pm$ studied in Ref. [1], especially considering the fact that our parton level analysis overestimate the signal by a factor of 2 [compare the

⁶Please notice the arrow in Fig. 4 to indicate the maximum value of the signal at $\cos\phi \approx 1$.

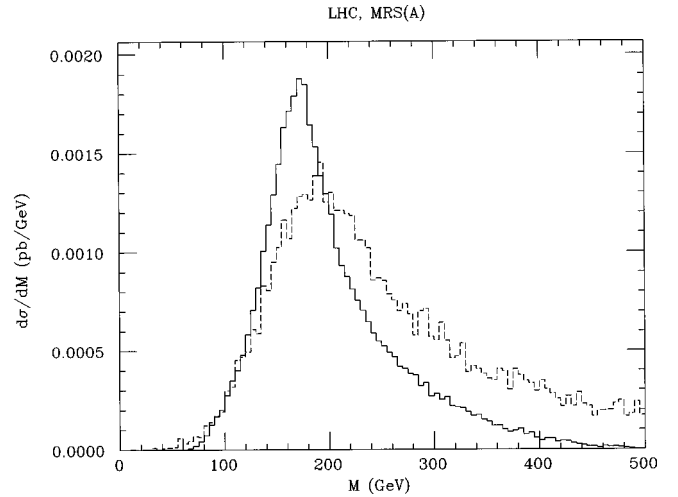


FIG. 5. Differential distributions in the estimated invariant mass of the $\ell\ell'+\bar{\nu}_\ell\nu_{\ell'}$ system for the Higgs signal ($M_H=170$ GeV, solid histogram) and the single-top-quark background (dashed histogram) at the LHC after the acceptance cuts (1)–(6). The parton distribution functions used are MRS(A). Note that the background rates have been divided by 2 in order to facilitate the comparison between the two curves.

numbers in our Table I to those in Tables I and II of Ref. [1] in response to the application of cut number (7)], while more accurately predicting the background rates. Finally, one should notice the effectiveness of the selection strategy based on the cuts (1)–(11) against events of the type (1), as the overall reduction factor on this background is above 1000.

IV. SUMMARY AND CONCLUSIONS

In this paper, we have studied the yield of process $bg \rightarrow tW^\pm \rightarrow bW^+W^- \rightarrow b\ell^+\ell'^-\nu_\ell\bar{\nu}_{\ell'}$ (where $\ell, \ell' = e, \mu$)

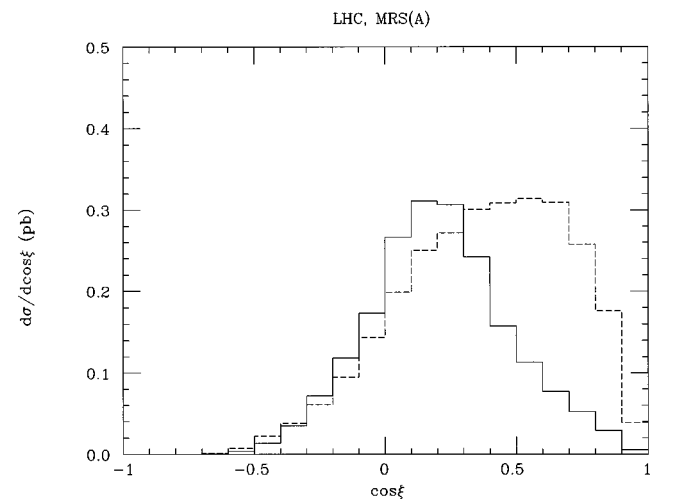


FIG. 6. Differential distributions in the angle between the lepton with highest transverse momentum, boosted to the dilepton rest frame, and the momentum vector of the dilepton system itself for the Higgs signal ($M_H=170$ GeV, solid histogram) and the single-top-quark background (dashed histogram) at the LHC after the acceptance cuts (1)–(6). The parton distribution functions used are MRS(A). Note that the background rates have been divided by 2 in order to facilitate the comparison between the two curves.

TABLE I. The expected signal and background number of events for 5 fb^{-1} at the LHC after the application of the selection criteria discussed in the text. Only the two-body decays $W^\pm \rightarrow \ell \bar{\nu}_\ell$ with $l = e, \mu$ are considered in both signal and background. The parton distribution functions used are MRS(A).

Process $pp \rightarrow X$	Accepted event rates							
	No cut	Cuts (1)–(3)	Cuts (4)–(6)	Cut (7)	Cuts (8)–(9)	Cut (10)	Cut (11)	
$gg \rightarrow H \rightarrow W^+ W^-$								
$M_H = 155 \text{ GeV}$	1832	1032	893	893	209	147	70	
$M_H = 160 \text{ GeV}$	2002	1154	1035	1035	267	208	109	
$M_H = 165 \text{ GeV}$	2017	1179	1054	1054	270	219	119	
$M_H = 170 \text{ GeV}$	1929	1141	988	988	244	199	99	
$M_H = 175 \text{ GeV}$	1829	1087	901	901	215	176	79	
$M_H = 180 \text{ GeV}$	1702	1019	801	801	184	152	61	
$bg \rightarrow tW^\pm \rightarrow bW^+ W^-$	13408	8254	2794	238	44	42	13	
$\sqrt{s} = 14 \text{ TeV}$		$\mathcal{L} = 5 \text{ fb}^{-1}$			$m_t = 175 \text{ GeV}$			
			MRS(A)					

as ‘‘irreducible’’ background to the $gg \rightarrow H \rightarrow W^+ W^- \rightarrow \ell^+ \ell'^- \nu_\ell \bar{\nu}_{\ell'}$ signature of the standard model Higgs boson, which has recently been claimed as the most viable channel to detect such a scalar in the mass range $155 \text{ GeV} \lesssim M_H \lesssim 180 \text{ GeV}$ at the Large Hadron Collider. Although we have confined ourselves to the parton level only, we believe we have performed a consistent signal-to-background analysis, exploiting the same event selection procedure advocated in literature. (In particular, the shape of the parton level distributions used to disentangle the signal from the irreducible $W^+ W^- X$ noise resembles very closely those previously obtained at hadron level.) This has enabled us to assess that nonresonant $W^+ W^- X$ events due to single-top-quark production via bg fusion are rather numerous and comparable to the rates of any of the reactions gg , $q\bar{q} \rightarrow t\bar{t}$, $gg \rightarrow tbW^\pm$, and $gg, q\bar{q} \rightarrow W^+ W^-$, which have in fact been shown to represent the largest components of the total background to the Higgs boson detection channel in two charged leptons and missing energy and momentum. In contrast, $bg \rightarrow bW^+ W^- \rightarrow b\ell^+ \ell'^- \nu_\ell \bar{\nu}_{\ell'}$ events not proceeding via single-top-quark diagrams are negligible. Therefore, we think that the production process $bg \rightarrow tW^\pm$ that we have studied should be included in the experimental Monte Carlo simulations which will be used in order to confirm or disprove the existence of the Higgs scalar of the standard model

in the above mass range at the CERN proton-proton collider. We believe this to be particularly important, as the discussed signature does not allow one to reconstruct the narrow Higgs resonance (because of the neutrinos escaping the detectors). In fact, the presence of the latter will be established by an ‘‘event-counting’’ operation over a rather broad region in mass, where the $H \rightarrow W^+ W^-$ signal and the $bg \rightarrow tW^\pm$ background have a very similar shape. For the purpose of aiding future analyses, we make available upon request the electronic version of the matrix element for $bg \rightarrow bW^+ W^- \rightarrow b\ell^+ \ell'^- \nu_\ell \bar{\nu}_{\ell'}$.

However, we would like to conclude this study by stressing that the inclusion of the single-top-quark background in tW^\pm events will certainly not spoil the chances of detecting the standard model Higgs in the advocated decay channel and that the exploitation of the two charged leptons and missing energy signature remains crucial in Higgs searches at hadron colliders.

ACKNOWLEDGMENTS

We thank Bryan Webber for reading the manuscript and for useful comments and Herbi Dreiner for his assistance with the bibliography of process (1). We are grateful to the UK PPARC for financial support.

- [1] M. Dittmar and H. Dreiner, Phys. Rev. Lett. **55**, 167 (1997).
- [2] M. Dittmar and H. Dreiner, presented at the Ringberg Workshop ‘‘The Higgs Puzzle—What can We Learn from LEP2, LHC, NLC, and FMC?,’’ Ringberg, Germany, hep-ph/9703401, 1996.
- [3] CMS Technical Proposal, CERN/LHC/94-43 LHCC/P1, 1994.
- [4] ATLAS Technical Proposal, CERN/LHC/94-43 LHCC/P2, 1994.
- [5] T. G. Rizzo, Phys. Rev. D **22**, 722 (1980); W.-Y. Keung and W. J. Marciano, *ibid.* **30**, 248 (1984).

- [6] J. Fleischer and F. Jegerlehner, Phys. Rev. D **23**, 2001 (1981); B. A. Kniehl, Nucl. Phys. **B357**, 439 (1991).
- [7] E. W. N. Glover, J. Ohnemus, and S. D. Willenbrock, Phys. Rev. D **37**, 3193 (1988).
- [8] *Proceedings of the ECFA Large Hadron Collider Workshop*, Aachen, Germany, 1990, edited by G. Jarlskog and D. Rein (CERN Report No. 90-10, ECFA Report No. 90-133, Geneva, Switzerland, 1990).
- [9] V. Barger, G. Bhattacharya, T. Han, and B. A. Kniehl, Phys. Rev. D **43**, 779 (1991).

- [10] T. Sjöstrand, CERN-TH 7112/93; *Comput. Phys. Commun.* **39**, 347 (1986); T. Sjöstrand and M. Bengtsson, *ibid.* **43**, 43 (1987).
- [11] R. J. N. Phillips, P. M. Zerwas, and J. Zunft, in *Proceedings of the ECFA Large Hadron Collider Workshop* [8].
- [12] A. P. Heinson, A. S. Belyaev, and E. E. Boos, *Phys. Rev. D* **56**, 3114 (1997).
- [13] A. P. Heinson, presented at “31st Rencontres de Moriond: QCD and High-energy Hadronic Interactions,” Les Arcs, France, hep-ex/9605010, 1996.
- [14] H. Georgi, S. L. Glashow, M. E. Machacek, and D. V. Nanopoulos, *Phys. Rev. Lett.* **40**, 692 (1978).
- [15] M. Djouadi, M. Spira, and P. M. Zerwas, *Phys. Lett. B* **264**, 440 (1991).
- [16] S. Dawson, *Nucl. Phys.* **B359**, 283 (1991).
- [17] S. Dawson and R. P. Kauffman, *Phys. Rev. D* **49**, 2298 (1993).
- [18] A. Djouadi, M. Spira, and P. M. Zerwas, *Phys. Lett. B* **311**, 255 (1993); K. Melnikov and O. Yakovlev, *ibid.* **312**, 179 (1993); M. Spira, in *Proceedings of the “Ringberg Workshop on Electromagnetic Interactions,”* Ringberg, Germany, 1995, p. 203; D. Graudenz, in *Proceedings of the “30th Rencontres de Moriond: QCD and High Energy Hadronic Interactions,”* Meribel les Allues, France, 1995, p. 65; M. Spira, A. Djouadi, D. Graudenz, and P. M. Zerwas, *Nucl. Phys.* **B453**, 17 (1995).
- [19] F. Halzen and C. S. Kim, *Int. J. Mod. Phys. A* **2**, 1069 (1987).
- [20] G. A. Ladinsky and C.-P. Yuan, *Phys. Rev. D* **43**, 789 (1991).
- [21] M. Duncan, G. L. Kane, and W. Repko, *Nucl. Phys.* **B272**, 517 (1986); G. L. Kane and C.-P. Yuan, *Phys. Rev. D* **40**, 2231 (1989).
- [22] T. Stelzer and W. F. Long, *Comput. Phys. Commun.* **81**, 357 (1994).
- [23] H. Murayama, I. Watanabe, and K. Hagiwara, HELAS: Helicity Amplitude Subroutines for Feynman Diagram Evaluations, KEK Report No. 91-11, 1992.
- [24] G. P. Lepage, *J. Comput. Phys.* **27**, 192 (1978).
- [25] C. Becchi, A. Rouet, and R. Stora, *Ann. Phys. (N.Y.)* **98**, 287 (1976); G. J. Gounaris, R. Kogerler, and H. Neufeld, *Phys. Rev. D* **34**, 3257 (1986).
- [26] Z. Kunszt, S. Moretti, and W. J. Stirling, *Z. Phys. C* **74**, 479 (1997).
- [27] S. Moretti, DFTT 79/95, Cavendish-HEP-95/18, DTP/95/104, hep-ph/9612310, 1996.
- [28] A. D. Martin, R. G. Roberts, and W. J. Stirling, *Phys. Rev. D* **50**, 6734 (1994).
- [29] A. D. Martin, R. G. Roberts, M. G. Ryskin, and W. J. Stirling, DTP/96/102, hep-ph/9612449, 1996.
- [30] A. D. Martin, R. G. Roberts, and W. J. Stirling, *Phys. Lett. B* **354**, 155 (1995).
- [31] A. D. Martin, R. G. Roberts, and W. J. Stirling, *Phys. Lett. B* **387**, 419 (1996).
- [32] P. Grannis, in *Proceedings of the International Conference on High Energy Physics*, Warsaw, Poland, 1996, edited by Z. Ajduk and A. Wroblewski (World Scientific, Singapore, 1997).